Thieken, A. H., Apel, H., Merz, B. (2015): Assessing the probability of large-scale flood loss events - a case study for the river Rhine, Germany. - *Journal of Flood Risk Management*, *8*, 3, p. 247-262.

DOI: http://doi.org/10.1111/jfr3.12091

FOR PUBLICATION IN THE JOURNAL OF FLOOD RISK MANAGEMENT

Revised version of Manuscript ID: JFRM-0145-12

ASSESSING THE PROBABILITY OF LARGE-SCALE FLOOD LOSS EVENTS – A CASE STUDY FOR THE RIVER RHINE, GERMANY

Annegret H. Thieken[1*], Heiko Apel[2], Bruno Merz[2]

[1]University of Potsdam, Institute of Earth and Environmental Sciences, Karl-Liebknecht-Strasse 24-25, D-14476 Potsdam, Germany

[2]GFZ German Research Centre for Geosciences, Hydrology Section, Telegrafenberg, D-14473 Potsdam, Germany

*Corresponding author:

Prof. Dr. Annegret Thieken, thieken@uni-potsdam.de, phone: +49-331-977-2984

ABSTRACT

Flood risk analyses are often estimated assuming the same flood intensity along the river reach under study, i.e. discharges are calculated for a number of return periods T, e.g. 10 or 100 years, at several streamflow gauges. T-year discharges are regionalised and then transferred into T-year water levels, inundated areas and impacts. This approach assumes that (1) flood scenarios are homogeneous throughout a river basin, and (2) the T-year damage corresponds to the T-year discharge. Using a reach at the river Rhine, this homogeneous approach is compared to an approach that is based on four flood types with different spatial discharge patterns. For each type, a regression model was created and used in a Monte-Carlo framework to derive heterogeneous scenarios. Per scenario, four cumulative impact indicators were calculated: 1) the total inundated area, 2) the exposed settlement and industrial areas, 3) the exposed population, and 4) the potential building loss. Their frequency curves were used to establish a ranking of eight past flood events according to their severity. The investigation revealed that the two assumptions of the homogeneous approach do not hold. It tends to overestimate event probabilities in large areas. Therefore, the generation of heterogeneous scenarios should receive more attention.

KEYWORDS: flood risk analysis, frequency analysis, discharge pattern, exposure, damage estimation, population density, land-use, Rhine, Germany

1. INTRODUCTION

Flood risk analyses are an essential element of an integrated flood risk management approach and the basis for effective risk mitigation decisions. Since risk is understood as a product of damage and probability, a typical scenario set for a flood risk analysis should contain scenarios that cover the whole range of possible flood discharges and associated probabilities as well as estimates on potential consequences in the region under study (Kaplan and Garrick 1981; Merz et al. 2009). Following this concept, a flood hazard event which describes the discharges and inundations along a river reach is distinguished in this paper from a flood loss event that sums up the cumulative flood impacts in the affected area.

In small catchment areas, a set of flood hazard events is basically produced by two steps: (1) estimating the T-year discharge along the watercourse (where T quantifies the return period of the discharge), and (2) transferring the flood discharges into water levels and inundated areas which serve as input for a consecutive flood impact analysis. In such an approach, the T-year scenario is composed of all inundated areas along the river reach, which result from the T-year discharge at that location. In most studies, these scenarios are the result of a flood frequency analysis, i.e. the application of extreme value statistics to a record of observed flood discharges at the gauges of interest (e.g. Stedinger et al. 1992). In many cases, (local) on-site frequency analysis is complemented by regional flood frequency analysis, using data from gauging stations that are supposed to have similar flood behaviour (e.g. Hosking and Wallis 1997). In the second step, different hydraulic modelling techniques have been used, such as 1D hydrodynamic simulation for compact and coherent river reaches (e.g. Büchele et al. 2006). For river sections with dikes, which may fail as consequence of extreme discharges, more complex simulation approaches may be chosen, such as coupled 1D-2D hydraulic models (e.g. Vorogushyn et al. 2010).

Combining the inundated area with a loss model delivers a quantification of potential impacts leading to a quantitative description of a flood loss event. For example, the Rhine-Atlas provides an overview of the flood situation and direct tangible damages along the river for the 10-year, the 100-year and an extreme scenario at a scale of 1 : 100 000 (ICPR 2001). Similar examples are presented by te Linde et al. (2011) or in hazard and risk maps that become more and more widespread due to the requirements of the European Flood Directive (EC/2007/60). These maps show homogeneous flood situations with equal return periods which are, however, rarely found in reality, particularly in large areas.

An analysis of flood hazard events along the river Rhine and in the whole of Germany revealed that there is considerable variation in the return periods of discharges that occur during an event within a river basin (Lammersen et al. 2002; Merz et al. 2005; Uhlemann et al. 2010). Merz et al. (2005) demonstrated that the coefficient of variation of return periods from different gauges increased for a particular event with an increasing mean return period of that event. The spatial variation of discharges in a catchment and their associated return periods depend on the space-time patterns of meteorological, hydrological and hydraulic processes. These are influenced by various characteristics: whereas some are constant between events (e.g. geomorphology of sub-catchments, river training and retention measures), others vary from event to event (e.g. spatial soil moisture distribution at the beginning of the flood). For example, the return period downstream of the confluence of two rivers depends on the temporal superposition of the two flood waves. If the peaks of the flood waves of the two rivers arrive at the same time, the return period downstream of the confluence will be higher than in case of temporarily shifted flood waves. In the Rhine catchment, this effect was observed after the construction of four weirs between Marckolsheim and Iffezheim at the Upper Rhine between 1955 and 1977. Prior to 1955, the flood wave of the tributary river Neckar normally preceded the flood wave coming from the Upper Rhine. The river training measures, however, accelerated flood wave propagation in the Upper Rhine and further resulted in an increased probability that a flood peak of the Upper Rhine coincides with the flood peak of the tributary river Neckar, ultimately leading to an increased flood hazard and risk downstream of confluence of Rhine and Neckar (Lammersen et al. 2002).

In large catchments the use of an equal return period throughout the whole catchment must thus be questioned and restricts the use of scenarios that were derived by the on-site approach described above (further referred to as homogeneous scenarios) to applications where local information is needed (Table 1). However, for some applications flood hazard scenarios are needed which are based on realistic large-scale spatial patterns of flood discharges and their return periods. Particularly reinsurers and national disaster managers demand for such flood scenarios, their extent, impacts and probabilities. Worst-case scenarios or probable maximum losses (PML) are needed to design and assess risk transfer systems, e.g. in order to assess and ensure solvency of (flood) insurers and (re-)insurers or to negotiate about a mandatory flood insurance as happened in Germany after the severe flood event in 2002 (Schwarze and Wagner 2004).

Table 1: Some areas of use of scenarios and the required information

Use/Application of scenarios	**Required information**
Building insurance, homeowners and companies	Building-specific statements about the flood hazard (e.g. hazard zones of the 10 to 200-year floods)
Local disaster management	Local scenarios including extraordinary situations
Flood design (dams)	Site-specific statements on extreme discharges (e.g. 10 000-year flood), including risk of dam failure
Federal disaster management	Large-scale, extraordinary scenarios that cannot be handled by regional agencies
Re-insurance	Probable maximum flood (large events) and potentially resulting losses from the insurance portfolios

1.1 Objectives of this paper

The scientific literature on methodologies how to create realistic heterogeneous flood scenarios and to assess their probability is not well developed (see section 1.2 for a brief review). Therefore, the main aim of this paper is to introduce a methodology that allows estimating the probability of flood loss events in large areas. For this purpose, a probabilistic approach for the generation of realistic flood hazard scenarios is presented and combined with a flood impact analysis, in which four indicators for flood impacts are considered. Their frequency distributions were finally used to estimate probabilities of flood (loss) events.

For the investigation, a reach along the river Rhine was chosen (see Fig, 1), where an area of 14 600 km² is at risk of being flooded assuming an extreme scenario with 200 to 500-year flood discharges along the whole reach (ICPR 2001). This area covers total property and infrastructure assets of Euro 750 000 million based on depreciated values and market prices as at 2001. Direct economic losses were estimated to be Euro 165 000 million for the extreme scenario along the whole river Rhine. According to ICPR (2001), 83% of the estimated losses were assigned to settlement areas that only accounted for 11% of the area modelled to be affected by the extreme scenario. However, it will be shown below that past flood events only affected certain reaches of the river Rhine. The estimates of ICPR (2001) as well as of te Linde et al. (2011) are based on homogeneous scenarios. Therefore, a second aim of this paper is to compare the probabilities of real (heterogeneous) flood scenarios with homogeneous scenarios that assume constant return periods of discharges along the whole river reach.

1.2 Determining the T-year flood event in large areas – a literature review

Analogous to flood frequency analysis, event probabilities could be derived from a distribution of an indicator that summarises the event hazard magnitude for the whole region under study. In principle, such a cumulative indicator could be calculated either on the basis of an aggregated multi-site discharge analysis (addressing the hazard) or by a flood impact analysis (considering impacts and losses).

Although there is a huge body of literature on flood frequency analysis, e.g. the suitability of different distribution functions and data series or parameter estimation methods, methods for an aggregated multi-site discharge analysis are lacking. Only recently, there have been first applications of multi-variate distribution functions to describe the joint probability of flood peaks at multiple sites. For example, Ghizziani et al. (2010, 2012) applied the multi-variate skew-t-distribution and the Student copula to the Tarano basin, Italy, and the Upper Mississippi River, respectively. A similar approach was developed by Keef et al. (2009a, 2009b) based on the spatial dependence model of Heffernan and Tawn (2004). It derives the statistical dependence structure between river gauges using the entire series of daily flow data under the condition that one gauge exceeds a threshold. It can be used to generate synthetic scenarios of large-scale flood peaks. Although these multi-variate hazard approaches are promising, they are taken up only very slowly in flood risk research and practice due to their complexity.

Another promising approach is the quantification of the event magnitude by an impact indicator. In fact, a frequency analysis of a time series of annual flood losses in a large area would enable us to assign a probability to each event of such a series. In practise, however, time series of losses are hardly available, contain many zero values, i.e. years without or only low losses that might cause a bias in the risk estimates (Arnell 1989), or data use is limited due to data inconsistencies. The latter can be caused by temporal changes of land use and assets in the flood-prone areas, implemented prevention measures as well as altered methods for damage reporting. In addition, the type of impact indicator and the data source might influence the result. Poor quality of damage data is frequently reported (e.g. Downton and Pielke 2005; Gall et al. 2009; Kron et al. 2012) and improvements have constantly been demanded (e.g. Ramirez et al. 1988; Mileti 1999; Handmer et al. 2005; Greenberg et al. 2007; Merz et al. 2010; Elmer et al. 2010; Bubeck et al. 2012). Although the lack of reliable, consistent and comparable data is seen as a major obstacle for risk analyses and effective and long-term loss prevention (e.g. Changnon 2003; Downton and Pielke 2005), consistent flood loss data bases are still missing.

To overcome these data problems, a scenario set of possible flood events could be synthetically generated and coupled with a flood impact model, e.g. a flood loss estimation model, in order to derive consistent estimates of the flood impacts. If the scenarios are generated properly, i.e. their probabilities are estimated on an annual basis, a frequency analysis of the simulated cumulative impact indicator could be performed in order to derive event probabilities.

Flood losses result from a chain of processes (see Gouldby et al. 2005), starting with the triggering rainfall event (source), consecutive runoff processes in the catchments and wave propagation in the hydraulic network (pathways) leading to inundation of properties (receptors) and eventually damage (consequences).

In flood risk models either the whole process chain or a reduced chain can be simulated. The crucial point for the generation of a probabilistic scenario set is where probability is introduced. Rainfall or discharge data are commonly used for this purpose. For example, van Dyck and Willems (2013) used the rate and spatial extent of severe precipitation with information on topography, river networks as well as flooded areas and aggregated losses of historical flood events to estimate the probabilistic flood risk in large areas; the approach was demonstrated in Belgium.

Based on ideas of USACE (1999), Apel et al. (2004, 2006) developed a dynamic-probabilistic model and applied it to the Lower Rhine in Germany. Their approach combined the flood frequency curve at the Cologne gauge with simplified flood process models for wave propagation, dike breaches and inundation in a Monte Carlo framework. The simplifications enabled them to simulate a large number of hazard scenarios and to derive frequency distributions downstream (at the Rees gauge) that also accounted for dike breaches and associated uncertainties.

Rodda (2005) described the development of a flood risk model for main rivers in the Czech Republic and its application for (re-)insurance purposes. The model included the generation of 30 synthetic (discharge) events, the conversion of discharges into water levels and inundation areas as well as a calculation of insured losses. The flood hazard events were generated directly from discharge data. Spatial distributions of the ratio between the peak flood discharge and the median annual flood (Q/Q2) were used to identify three distinct patterns that served as a basis to generate 30 events. Initial flood magnitudes were further modified by random factors. Since no stochastic approach was used to generate scenarios, a probabilistic analysis of the resulting losses was, however, not possible (Rodda 2005). In an earlier work, Rodda and Berger (2002) introduced a stochastic approach for the generation of flood hazard events in the UK. Here, a stochastic event set of more than 2000 flood-inducing rainfall events was coupled dynamically with a runoff model and a hydraulic model was used to determine maximum flood extent and depth. Flood risk was finally given in terms of insured building loss over the full range of possible return periods. A similar approach was used by te Linde et al. (2010) to investigate impacts of climate change and management strategies on flood risk in the Rhine catchment. None of these approaches, however, investigated flood loss event probabilities, which are addressed in this paper.

2. METHODOLOGY

A probabilistic model was developed in order to generate realistic, heterogeneous flood hazard scenarios as well as to estimate potential impacts and flood loss event probabilities. The model development comprised the following steps:

1) Statistical analysis of discharges at gauges on the river reach under study;

2) Probabilistic generation of discharge pattern for the study area (flood hazard events);
3) Transformation of discharges into water levels and inundation areas;
4) Determination of flood impacts; and
5) Estimation of the flood loss scenario/event probability.

The steps 3 to 5 were also applied to eight past flood events and four homogeneous flood scenarios. All modules are introduced in the next sections.

2.1 Statistical analysis of flood discharges

Mean daily discharges from 1931 to 1999 were analysed at seven gauges between Maxau, a gauge located near the city of Karlsruhe, and Rees, located at the German-Dutch border (Fig. 1). The river reach under study covers parts of the Upper, Middle and the Lower Rhine. At first, a series of annual maximum discharges (AMS) was derived for each gauge. Independency of the events was tested as recommended by DVWK (1999). The frequently applied, recommended and found to be suitable GEV-distribution (see e.g. Vogel et al. 1993, Vogel and Wilson 1996, Castellarin et al. 2012) was fitted to each AMS using L-moments as given in Hosking and Wallis (1997).

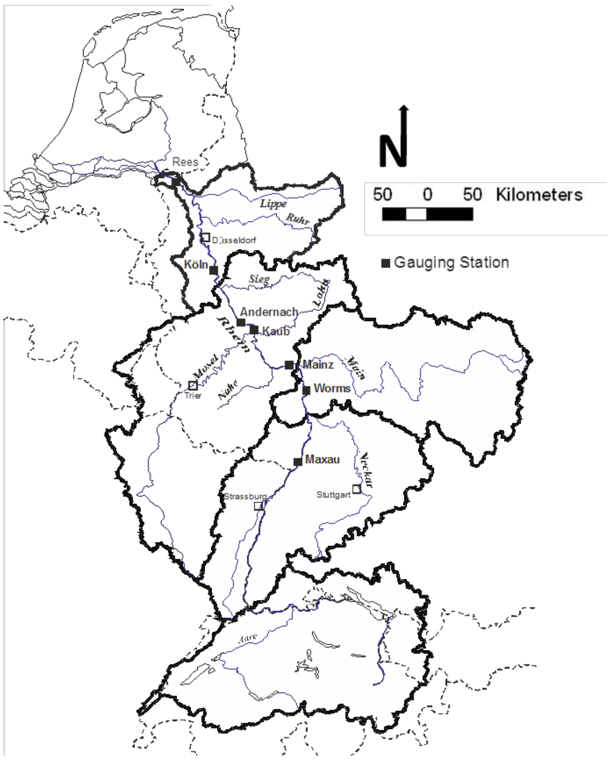

Fig. 1: Rhine Catchment and the locations of discharge gauges.

The AMS of the seven gauges served as a starting point for the generation of a flood hazard event set: For each flood event that was included in an AMS of at least one gauge, the maximum discharge that could be attributed to this event was determined at all other gauges. In this way, a data set with 120 events was generated. Each event contained the maximum discharges that were observed at the seven gauges.

In order to be consistent with the length of the observation period, only the 69 largest events were selected. For this, a cumulative discharge indicator was introduced. In a first step, the discharges of the event set were normalized by dividing them by the median discharge of the corresponding AMS. Then the normalized discharges of all gauges were summed up for each event using a weight that reflects the incremental increase in the median discharge at each gauge (see Table 2). All events were sorted by this indicator in descending order and the first 69 events, i.e. 57.5 % of the initial events, were chosen for further analysis.

Since past flood events at the river Rhine revealed that the spatial distribution of flood discharges is heterogeneous and depends on the centre of the flood, i.e. typical floods at the Upper Rhine can be distinguished from typical floods at the Middle or Lower Rhine (see Disse and Engel 2001; Lammersen et al. 2002; Merz et al. 2005; and section 3.1), the correlation between discharges from different gauges tends to decrease with increasing spatial distance. It was assumed that the correlations of discharges are higher if the event set is divided into more homogeneous subclasses. Therefore, all flood events were classified into four types. Besides Upper, Middle and Lower Rhine floods, a mixed flood type was considered (see data analysis in section 3.1). Subsequently, a regression model was derived for each flood type, i.e. linear regressions between a master gauge, which represented the centre of a flood of the respective type, and all other gauges were calculated (see section 3.1).

2.2 Probabilistic generation of discharge scenarios along the whole river reach

The results of the data analysis were used to generate heterogeneous discharge pattern. First, a flood type was randomly chosen. Then a discharge at the respective master gauge of the chosen flood type was sampled from its GEV distribution. Finally, the discharges at all other gauges were estimated by linear regressions.

Since regression functions do not reflect the total data variability, randomness was introduced to limit data smoothing that is inherent in regression: A normal distribution was assumed, in which the mean was taken from the linear regression between the master gauge and another gauge and the standard deviation reads as follows (after Cullen and Frey 1999; Apel et al. 2004):

$$\sigma_i = \sigma_{AMS(i)} \sqrt{1 - \rho_{i,m}{}^2}$$

where: σ_i: Standard deviation of residuals at gauge i

$\sigma_{AMS(i)}$: Standard deviation of the annual maximum series at gauge i

$\rho_{i,m}$: Correlation coefficient between gauge i and the master gauge m for the underlying flood type

For each scenario a random number between 0 and 1 was sampled from a uniform distribution and converted to σ_i using the equation above with, however, using the mean daily discharge of the whole time series 1931-1999 as lower limit to avoid negative values and systematic biases at the same time. Also, only one random number was sampled per scenario in order to prevent inexplicable discharge pattern. With this approach 100 discharge scenarios were generated, from which the 58 most severe scenarios measured by the cumulative discharge indicator were chosen for the flood impact analysis. This was done in order to generate scenarios on an annual basis. The share of 58 out of 100 scenarios is consistent with the 120 events in 69 years (see section 2.1). The number of scenarios was kept low in order to limit computation time for the consecutive inundation modelling.

2.3 Transformation of discharges to water levels and inundation areas

The flood impact analysis started with the conversion of flood discharges to inundated areas by a hydraulic transformation, i.e. discharges were converted to water levels using valid rating curves at the respective gauges. Further, water levels between the gauging stations were interpolated, and the flooded area was obtained by intersecting the interpolated water levels with a digital elevation model (DEM).

All calculations are based on the official DEM provided by the Federal Agency of Cartography and Geodesy with a grid cell size of 25 m and a vertical resolution of 0.01 m with a vertical accuracy of ± 10 cm in flat areas plus 5% of the grid cell size. At the gauge locations, river cross sections considering the whole flood plain and the dike hinterland were extracted from the DEM. To improve data quality, the river bed was corrected by additional data sources, such as official cross sections, mean water levels and gauge data. Rating curves were calculated at each gauge location on the basis of river cross sections and the Manning-Strickler-Equation assuming stationary conditions. At each gauge, discharges were then transformed into water levels, i.e. flood water levels above sea level. These were used in a linear directional interpolation along the main flow path, whose direction was derived from the centroids of the river as well as from additional cross sections. The resulting flood water levels were assigned to the (additional) cross sections and a triangular irregular network (TIN) was constructed. Finally, inundated areas were derived by a Cut/Fill-algorithm so that only adjacent grid cells were assigned as flooded. The water depths were calculated as difference between the DEM and the TIN. The algorithm was implemented in ArcGIS 9.0. It produced a grid data set containing the water depths as well as a table with the total inundated area and its volume, although the actual volume of the flood wave was not considered as boundary condition in the hydraulic transformation.

This method was used to derive inundated areas for 58 probabilistic discharge patterns (see sections 2.1 and 2.2). However, several small floods had a very similar discharge pattern. To further reduce computational efforts, the hydraulic transformation was only performed for scenarios where the 1-year flood discharge was exceeded at at least two of the seven gauges, as well as for two representative small flood scenarios (in total for 48 scenarios). Moreover, four homogeneous scenarios were calculated with the 10-, 20-, 50- or 100-year discharge at each gauge that were taken from the respective flood frequency distributions (AMS 1931-1999, GEV, L-Moments, see section 2.1). Finally, inundated areas were also determined for eight past flood events.

2.4 Quantification of flood impacts

Four indicators were used to estimate flood impacts:

1. the total inundated area,

2. the exposed, i.e. inundated, settlement and industrial area,
3. the exposed population, i.e. the number of residents in the inundated area, and
4. the direct monetary damage to residential buildings (building losses).

The size of the total inundated area was directly determined by the hydraulic transformation implemented in ArcGIS. To determine the inundated settlement and industrial areas, the water depth grid was intersected with a grid of the CORINE land cover data set as at 2000 (CLC2000; CORINE stands for Coordination of Information on the Environment). In the CLC2000 data set, settlement areas are represented by the land use codes 111 and 112, industrial areas and areas for transportation by the codes 121 to 124.

To estimate the flood-exposed number of residents, the inundation scenarios were intersected with the population map presented by Thieken et al. (2006). In general, census data on population are only provided for different administrative units, e.g. at the municipal level. With the help of CLC2000 data and the dasymetric mapping technique of Gallego (2001), Thieken et al. (2006) further disaggregated population within the municipalities leading to high-resolution data of population density. This map was further used to distribute municipal asset values provided by Kleist et al. (2006) resulting in a map with the unit asset value (in €/m²) for residential buildings (see Thieken et al. 2006).

To estimate the building loss, the asset map was combined with the meso-scale flood loss estimation model for the residential sector FLEMOps (Thieken et al. 2008). FLEMOps estimates building damage considering five water depth classes (≤ 20 cm, 21–60 cm, 61–100 cm, 101–150 cm, >150 cm above surface), three building types (i.e. one-family homes, (semi-)detached houses and multi-family homes) and two building qualities (i.e. low /medium and high quality). For all sub-categories, a mean building loss ratio was derived from empirical data of 1697 private households affected by the flood in August 2002 (see Büchele et al. 2006). Building losses in the different sub-categories were found to differ significantly on the level of $p<0.05$; this was tested by the Mann-Whitney-U-Test for two independent data groups and by the Kruskal-Wallis-H-Test for three or more subgroups (Büchele et al. 2006).

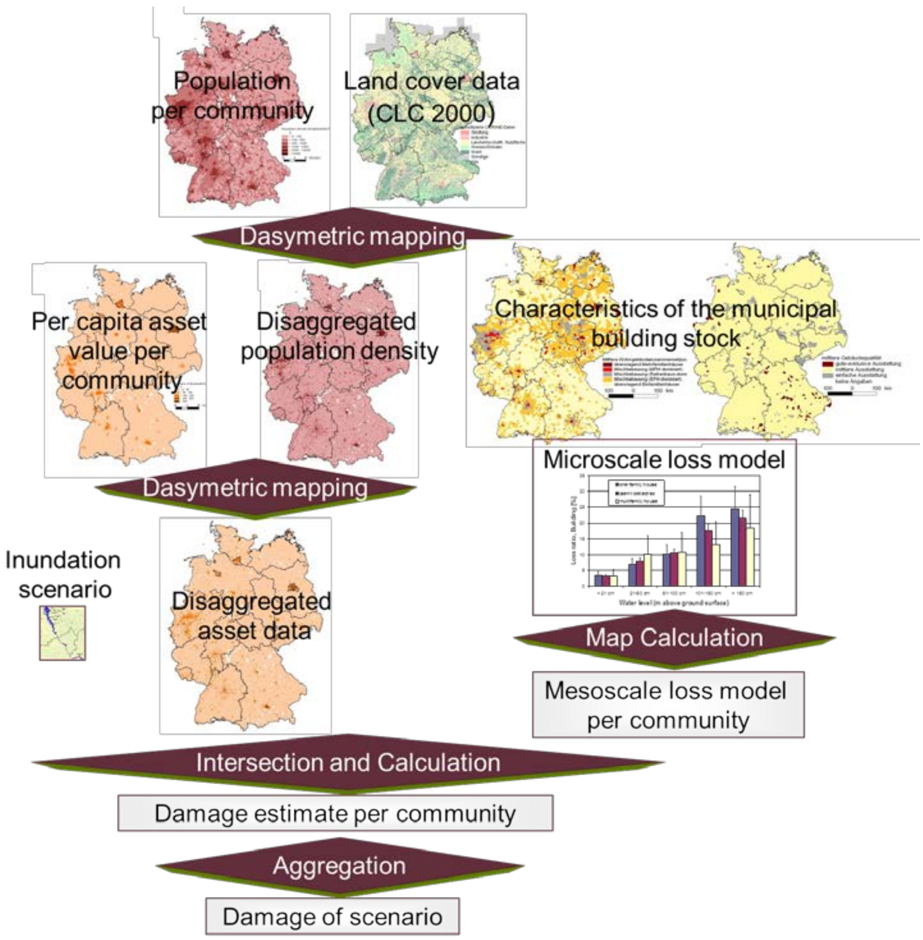

Fig. 2: The meso-scale Flood Loss Estimation Model for residential buildings (FLEMOps; Thieken et al. 2008).

In FLEMOps, these micro-scale damage functions were combined with a typical composition of residential building types on the municipal level and their mean building quality as illustrated in Fig. 2 and described by Thieken et al. (2008). For the loss estimation, each inundation scenario was first intersected with the map of unit residential asset values. Second, the financial loss was estimated by FLEMOps for each grid cell using its unit asset value, its water depth as well as the mean municipal building composition and quality. Finally, all grid estimates were summed up per scenario. Thieken et al. (2008) also introduced a second model stage (FLEMOps+) that accounts for effects of contamination and private precaution. However, due to lacking input data, this model stage was not applied in this study.

2.5 Estimation of the scenario/event probability

As described in sections 2.1 and 2.2, 58 out of 100 probabilistic discharge pattern scenarios were selected, but hydraulic transformation (section 2.3) and the flood impact analysis (section 2.4) were only performed for two representative small flood scenarios as well as for the 46 most severe scenarios. For the remaining 12 small flood scenarios, the flood impacts were estimated using exponential regression functions between the cumulative discharge indicator that was introduced in section 2.1 and each flood impact indicator. The exponential regressions yielded a $R^2 = 0.9361$, $R^2 = 0.9199$ and $R^2 = 0.9134$ for the estimated building damages, the exposed population and the affected land use types, respectively.

Furthermore, a GEV distribution was fitted to all 58 scenario estimates for each impact indicator. In a last step, these frequency distributions were used to estimate the return periods of eight past flood loss events (Fig. 3) and homogeneous flood scenarios, for which all four impact indicators were calculated, as well.

3. RESULTS AND DISCUSSION

3.1 Flood statistics and scenario generation

Mean daily discharges from 1931 to 1999 at seven gauges between Maxau and Rees (Fig. 1) were used to derive annual maximum discharge series (AMS; see Table 2). GEV distributions were used to estimate return periods of flood discharges for eight events that occurred between 1931 and 1999 (see Fig. 3). These events also illustrate the different flood types at the river Rhine. For example, the flood of November 1944 was almost limited to the Upper Rhine represented by the Maxau gauge, whereas in March 1988 intense flooding occurred particularly at the Middle Rhine represented by the Mainz gauge. In contrast, the Lower Rhine (see Cologne gauge) was severely affected in January 1995. Among the eight floods shown in Fig. 3, the February 1980 flood had the most homogeneous distribution of return periods. Remarkably, it was also the smallest of the eight flood events (Merz et al. 2005).

The different flood types are due to differences in the spatial distribution of the triggering rainfall events, varying antecedent conditions, the possible interplay with snowmelt and the convolution of flood waves from different tributaries. In general, the flow regime of the Upper Rhine is dominated by snowmelt and precipitation runoff from the Alps in the summer months. Further downstream the flow regime is mainly influenced by precipitation runoff from the uplands, where long lasting precipitation particularly occurs in winter (Disse and Engel 2001). These regimes result in different flood patterns: Within the AMS at the Maxau gauge half of the flood events occur during the summer months. This percentage drops to only 8% at the Cologne gauge (Merz et al. 2005).

For the scenario generation, all 69 flood events were assigned to one of four flood types: 1) Upper-Rhine-Floods (e.g. flooding in November 1994 and January 1955 in Fig. 3); 2) Middle-Rhine-Floods (e.g. flood in March 1988 in Fig. 3); 3) Lower-Rhine-Floods (e.g. flooding in January 1948, December 1993 and January 1995 in Fig. 3); and 4) a Mixed-Flood-Type (e.g. flooding in February 1980 and May 1983 in Fig. 3). From the 69 events selected for the analysis, approximately one third (i.e. 24 events) were classified as “Upper-Rhine-Flood”, followed by 18 “Lower-Rhine-Flood” events, 15 mixed floods and finally 12 “Middle-Rhine-Flood” events (Table 3).

Table 2: Statistics of the annual maximum series (AMS) at the discharge gauges at the river Rhine, discharges are given in m³/s. The weights reflect the incremental increase in the median discharge at each gauge and were used to calculate a cumulative discharge indicator (see section 2.1 for further explanation).

Gauge	Maxau	Worms	Mainz	Kaub	Andernach	Cologne	Rees
Time period	1931-1999	1937-1999	1931-1999	1931-1999	1931-1999	1931-1999	1931-1999
Mean	3007	3385	4007	4196	6251	6337	6579
Standard deviation	724	929	1189	1217	2030	2042	2122
Skewness	0.01	0.09	0.07	0.16	0.04	0.09	0.13
Curtosis	2.38	2.43	2.56	2.65	2.41	2.42	2.44
Minimum	1450	1510	1540	1600	2220	2270	2330
Maximum	4430	5400	6920	7160	10500	10800	11700
Median	2930	3440	4040	4240	6271	6340	6500
Weight	0.4508	0.0785	0.0923	0.0308	0.3125	0.0106	0.0246

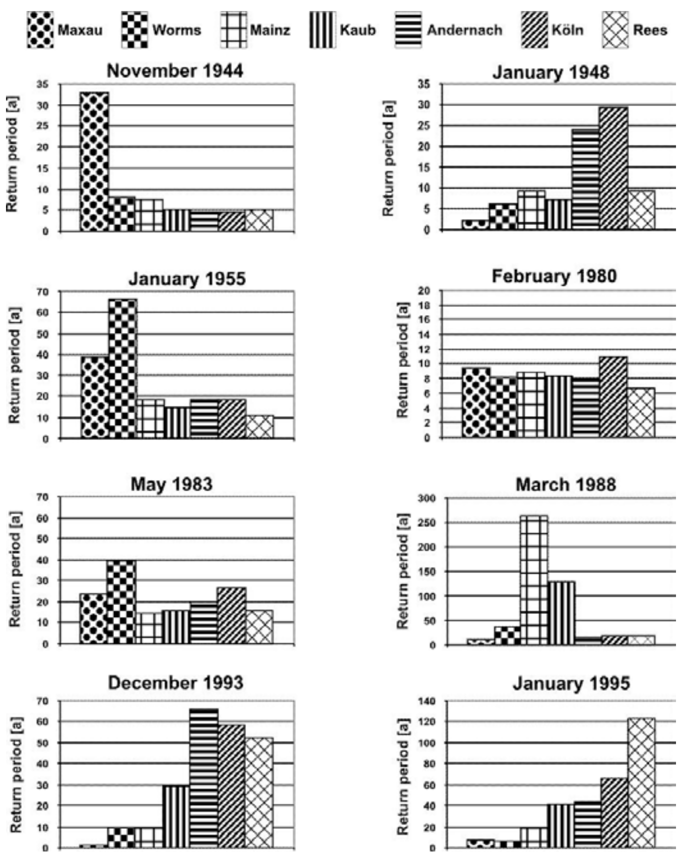

Fig. 3: Return periods of eight flood events at seven discharge gauges on the river Rhine. Return periods were estimated with the GEV on the basis of annual maximum discharge series from 1931 to 1999 (Source: Merz et al. 2005).

Table 3: Flood types of the river Rhine, their frequency and assigned master gauges.

Flood type	Occurrence of flood types in 69 events (1931-1999)	Master gauge
Upper Rhine Flood	35 % (24 events)	Maxau
Lower Rhine Flood	26 % (18 events)	Cologne
Middle Rhine Flood	17 % (12 events)	Mainz
Mixed Flood	22 % (15 events)	Mainz

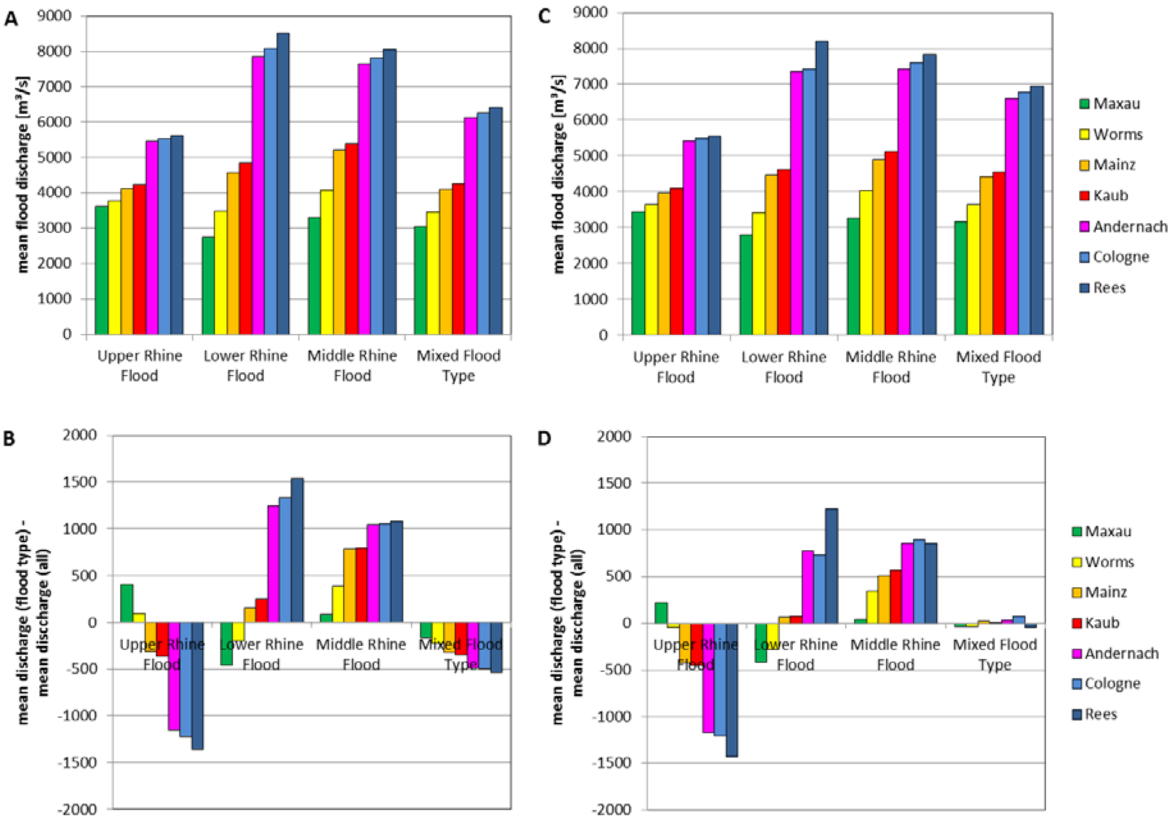

Fig. 4: Mean discharge pattern of the four flood types (A) and difference between the mean discharge per flood type and the mean discharge of all 69 events (B) as well as mean discharge pattern of the flood types in the 58 most severe scenarios (C) and their normalized discharge pattern (D).

In Fig. 4A, mean discharge patterns are shown per flood type. To better understand the difference between the four flood types, mean discharges per flood type were related to mean discharges of the whole event set (see Fig. 4B). The figure clearly reflects that the focal points of the flood types correspond well with the discharges of the respective gauges, i.e. in Upper-Rhine-Floods the discharges at Maxau and Worms are clearly above average, while discharges at the downstream gauges are below average. A contrary pattern is visible for Lower-Rhine-Floods. The pattern of Middle-Rhine-Floods is less clear, but in comparison to the other flood types the discharges at the gauges Mainz and Kaub are the highest above average. In the mixed flood type discharges at all seven gauges are below average.

As described in section 2.2, a correlation and regression analysis was performed for each flood type. Table 4 illustrates that the correlations between the gauge discharges are stronger for a distinct flood type than in the whole data set. Hence, the flood type classification improves the applicability of a regression model for the scenario generation. The consecutive regression analysis is only exemplarily illustrated in Fig. 5 for the gauges Cologne and Kaub.

As outlined in section 2.1 and 2.2, the regression model was used to generate discharge scenarios. In Fig. 4C and 4D the final set of 58 scenarios is compared to the original data of 69 events. In comparison to Fig. 4A and 4B, Fig. 4C and 4D reveal that the discharge pattern of generated Upper-Rhine-Floods and Middle-Rhine-Floods are similar to the observed ones, while the patterns of Lower-Rhine-Floods with a slightly underestimated discharges and the mixed floods with slightly overestimated could be further improved. This could be due to the small number of scenarios considered.

Table 4: Pearson's correlation coefficients between the flood discharges at seven gauges on the river Rhine for the whole data set (69 events) as well as for events of each of the four flood types. Significant correlations on the 0.01-level are highlighted with **, on the 0.05-level with *.

All 69 events	Maxau	Worms	Mainz	Kaub	Andernach	Cologne
Worms	0.77**					
Mainz	0.47**	0.82**				
Kaub	0.44**	0.81**	0.98**			
Andernach	0.14	0.59**	0.86**	0.88**		
Cologne	0.12	0.57**	0.84**	0.88**	1.00**	
Rees	0.08	0.51**	0.82**	0.85**	0.97**	0.98**
Upper-Rhine	Maxau	Worms	Mainz	Kaub	Andernach	Cologne
Worms	0.83**					
Mainz	0.79**	0.93**				
Kaub	0.77**	0.94**	0.99**			
Andernach	0.52*	0.75**	0.82**	0.83**		
Cologne	0.51*	0.75**	0.82**	0.83**	0.99**	
Rees	0.53**	0.72**	0.83**	0.82**	0.97**	0.98**
Lower-Rhine	Maxau	Worms	Mainz	Kaub	Andernach	Cologne
Worms	0.77**					
Mainz	0.71**	0.90**				
Kaub	0.74**	0.90**	0.95**			
Andernach	0.70**	0.92**	0.94**	0.96**		
Cologne	0.70**	0.88**	0.90**	0.95**	0.99**	
Rees	0.69**	0.77**	0.89**	0.91**	0.91**	0.92**
Middle-Rhine	Maxau	Worms	Mainz	Kaub	Andernach	Cologne
Worms	0.89**					
Mainz	0.86**	0.86**				
Kaub	0.87**	0.89**	0.99**			
Andernach	0.89**	0.86**	0.93**	0.93**		
Cologne	0.90**	0.90**	0.94**	0.94**	0.99**	
Rees	0.85**	0.89**	0.93**	0.94**	0.97**	0.98**
Mixed Flood	Maxau	Worms	Mainz	Kaub	Andernach	Cologne
Worms	0.95**					
Mainz	0.87**	0.90**				
Kaub	0.86**	0.91**	0.99**			
Andernach	0.77**	0.85**	0.92**	0.94**		
Cologne	0.78**	0.84**	0.93**	0.94**	0.99**	
Rees	0.73**	0.77**	0.91**	0.92**	0.96**	0.98**

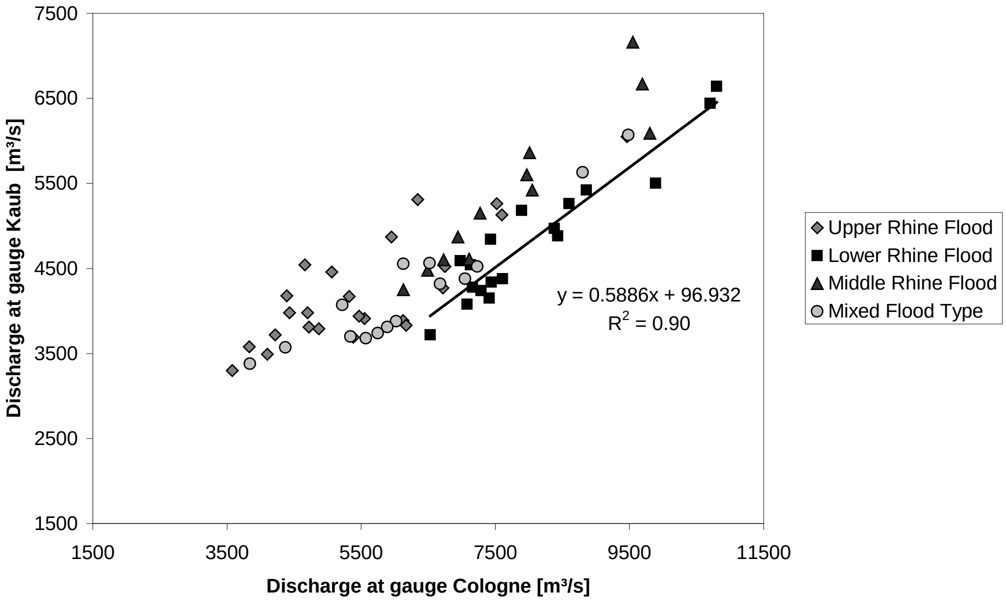

Fig. 5: Scatterplot of the discharges at the gauges Kaub and Cologne. A linear regression was calculated for events of the type “Lower Rhine Flood”.

3.2 Flood impact analysis

In the flood impact analysis, four indicators were calculated on the basis of inundation scenarios (see section 2.4). As an example, the inundated area of the flood event in December 1993 is shown in Fig. 6. Since no maps of the actual inundation extent in 1993 were available, the quality of the results is difficult to assess. However, owing to drawbacks of the hydraulic transformation as well as coarseness and errors of the DEM, the inundated areas tend to be overestimated. Particularly at the Lower Rhine the heights of embankments are not (well) represented in the DEM. Therefore, overtopping of embankments occurred at relatively low water levels resulting in huge inundated areas. Moreover, in flat lowland areas hydraulic transformation might result in unrealistic inundation extents, because the water volume of the inundated area is not limited by the volume of the flood wave. The presented scenarios have thus to be interpreted as worst-case scenarios.

Despite its drawbacks, this simple GIS-based hydraulic transformation was also used by Rodda (2005) and te Linde et al. (2011) for similar purposes. Apel et al. (2009) found that it can provide a good approximation of the inundated areas. Romanowicz and Beven (2003) emphasised that consistent and reliable information on floodplain geometry and infrastructure of the terrain is of utmost importance. Therefore, the analysis could be considerably improved by using better elevation data, particularly with regard to flood defence structures.

At the reach of the Lower Rhine in North-Rhine Westphalia a comparison of inundated areas with and without embankments was performed for a (homogeneous) 100-year, 200-year and 500-year flood by MURL (2000). The calculations were also based on a hydraulic transformation using, however, a 50 m DEM (with and without dikes) as input data. It was found that the total inundated area at the Lower Rhine was reduced to 22% to 28% when dikes were properly considered. The mean damage ratio, however, did not alter (MURL 2000). Therefore, it is assumed that the conclusions drawn from our modelling exercise are still valid even if the absolute impact estimates will change with better elevation data.

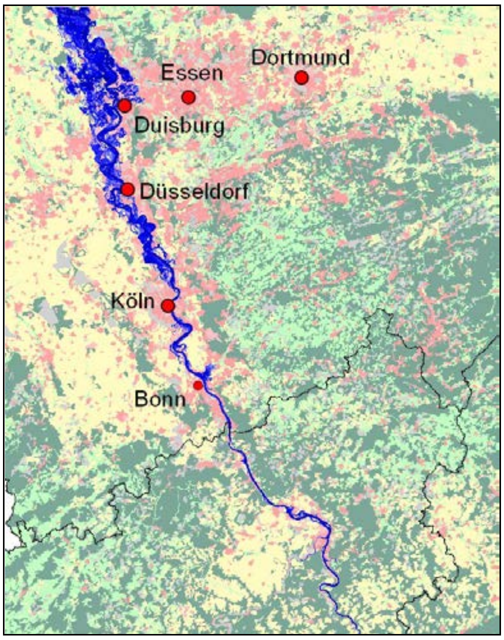

Fig. 6: Flood inundation scenario of the flood event in December 1993. Inundated areas are shown in blue, settlement areas in light red and industrial areas in grey.

Fig. 7 shows the frequency distributions of the four cumulative impact indicators. Except for the total inundated area, the course of the frequency distribution is very similar for all indicators. These frequency distributions were further used to estimate the return periods of the eight past flood events shown in Fig. 3. The results are summarised in Table 5. Besides the estimates based on the impacts the ranges of the return periods from on-site estimations of discharge using GEV are given in the last column of Table 5.

Although the return periods for each event differed depending on the impact indicator, the relative severity of the floods, i.e. their ranking, did not differ. According to this analysis, the flood in January 1995 was the most severe event with return periods between 115 and more than 200 years. It was followed by floods in December 1993, March 1988, May 1983, January 1955 and 1948 and February 1980. The lowest return period was assigned to the flood in November 1944, which was assessed as a 6- to 8-year event (Table 5). Table 5 reveals that the variation between the estimates increases with the severity of the event. Furthermore, the analysis demonstrates that – except for the three lowest events in January 1948, February 1980 and November 1944 – the range of estimated return periods based on the flood impacts was higher than the range of return periods based on on-site discharge frequency analyses (Table 5).

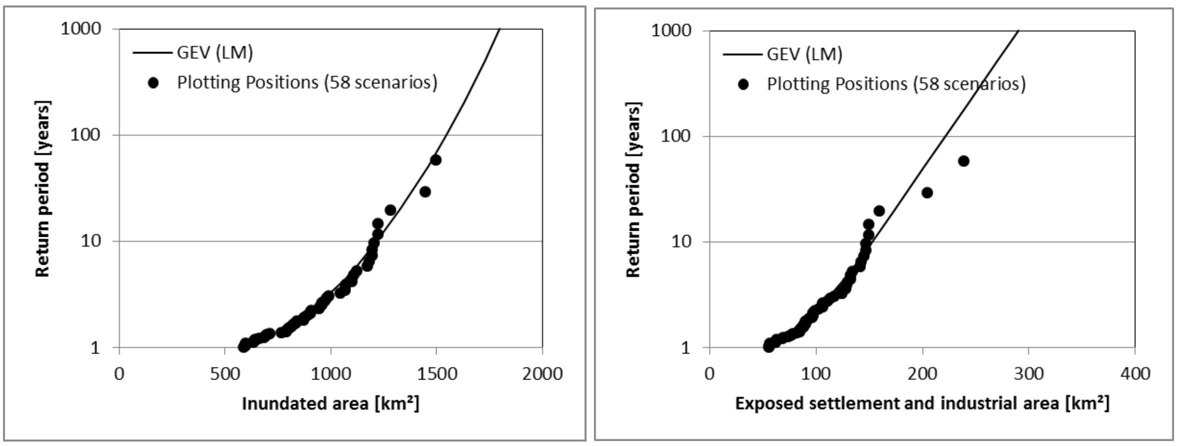

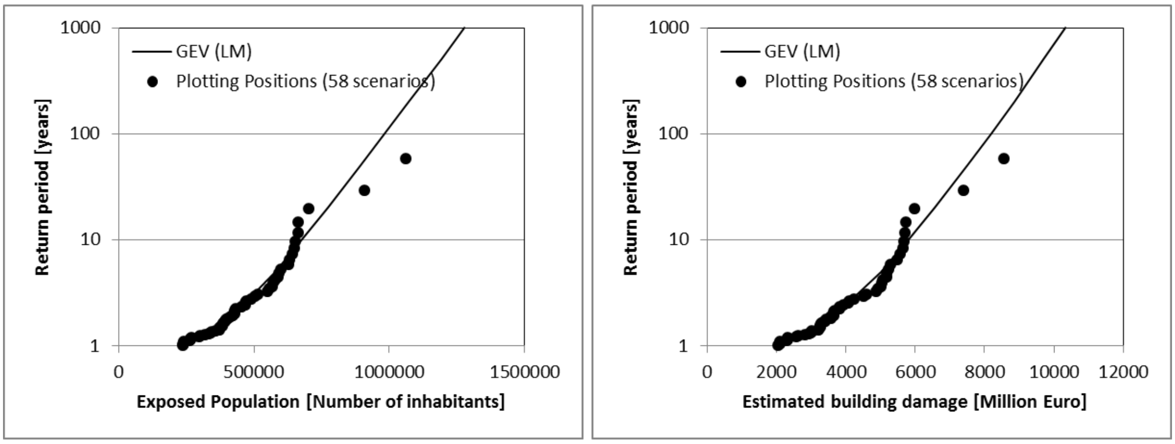

Fig. 7: Frequency distributions of the inundated area (A), exposed settlement and industrial area (B), exposed population (C) and potential damage to residential buildings (D).

It should be emphasized that this study did not aim to reanalyse the actual impacts of past flood events. Since data about land cover, population and residential asset values refer to the years 2000 or 2001, all results refer to these years. In fact, it was observed in many municipalities in the Rhine as well as in the adjacent Meuse catchment that the flood in January 1995 caused considerably lower damage than the event in 1993 despite higher discharges in many places (Wind et al. 1999; Grothmann and Reusswig 2006; Bubeck et al. 2012). This has commonly been attributed to better early warning and improved preparedness of affected people in 1995 (Wind et al. 1999). Bubeck et al. (2012) showed that private households considerably invested in mitigation measures after the 1993 flood and that this effect significantly reduced losses in 1995. In principle, the damage model FLEMOps is able to account for changes in private precaution, and validations showed that FLEMOps+ outperformed other stage-damage functions (Apel et al. 2009; Wünsch et al. 2009; Thieken 2011). Since the reanalysis of real losses was not the purpose of this paper, and due to lacking data, effects of precaution were, however, neglected in damage estimation. Still, it should be noticed that the approach helps to assess and compare the severity of different flood loss events by a consistent estimation of flood impacts.

Moreover, the return periods of four homogeneous flood hazard scenarios were estimated. In these scenarios the same return periods of the discharge were assumed along the whole river reach. The event probability of each scenario was again estimated by the frequency curves shown in Fig. 7. The results illustrate that the flood loss event return periods that were based on the cumulative impacts by far exceed the (constant) return period of the discharges (Table 6). The return period of the flood loss event was at least three times as high as the return period of the discharge, representing the flood hazard. The impact analysis reveals that a lower cumulative probability can be assigned to homogeneous hazard events, i.e. in our case, a return period of almost more than 100 years can be assumed for an event with constant 20-year flood discharges (Table 6).

In general, it has to be kept in mind that risk analyses are approximations to an unknown risk. Usually, risk statements on extreme events and their consequences cannot – or only partially – be validated in the traditional sense by comparing observed and simulated data, since such events have not been observed so far (Hall and Anderson 2002; Apel et al. 2008). Ideally, formal uncertainty analyses should be undertaken in order to better understand the system under study (Merz and Thieken 2009). Since input data and model choices influence the results, e.g. a large source of uncertainty of flood frequency analysis arises due to the choice of the distribution function (e.g. Merz and Thieken 2005), an uncertainty analysis of the presented modelling approach should be a next step.

Table 5: Return periods of the past eight flood events shown in Fig. 3 (single site and multi-site assessment).

Flood Event (ranked according to severity)	Event Return Period				Range of return periods of the discharges at all gauges (single site assessment; GEV) [years]
	Inundated area [years]	Exposed settlement and industrial area (CLC2000) [years]	Exposed population [years]	Potential building loss (FLEMOps) [years]	
January 1995	716	2025	1762	1522	7 … 123
December 1993	372	1091	1024	878	1 … 64

March 1988	291	298	366	399	9 … 262
May 1983	142	190	246	266	15 … 39
January 1955	100	92	117	125	11 … 67
January 1948	34	41	57	50	2 … 23
February 1980	18	14	17	17	7 … 9
November 1944	8	6	6	6	4 … 27

Table 6: Multi-site assessment of four homogeneous flood events (i.e. constant return periods along the river reach under study).

Scenario	Flood Loss Event Return Period				Return periods of the discharges at all gauges (single site assessment; GEV) [years]
	Inundated area [years]	Exposed settlement and industrial area (CLC2000) [years]	Exposed population [years]	Potential building loss (FLEMOps) [years]	
HQ10	35	36	45	45	10
HQ20	168	241	322	334	20
HQ50	1554	4134	2973	2824	50
HQ100	4450	NaN	7143	6306	100

4. CONCLUSIONS

Data analysis showed that the return periods of flood discharges considerably vary on the investigated reach of the river Rhine. Therefore, the conclusion that the return period of a flood discharge at a gauge is equal to the return period of the respective flood loss event is not always valid. Some applications in the (re-)insurance industry or on the national level need, however, to assess flood loss event probabilities even in large catchments. For such applications, heterogeneous flood hazard scenarios are needed. It was shown that heterogeneous flood hazard scenarios can be generated by combining flood type classification, flood frequency, correlation and regression analyses and hydraulic transformation. Loss event probabilities can be assessed by estimating cumulative flood impacts for the whole range of possible hazard scenarios. Suitable flood impact indicators are the total inundated (residential and/or industrial) area, the number of exposed residents or the potential building loss. In fact, only little difference was observed between the four indicators used in this study.

In our study area, the variation of return periods of cumulative flood impact indicators of real flood events is in most of the cases higher than the variation of return periods of the flood discharges at different gauges. In other study areas and timeframes this might be different.

The approach enabled us to establish a ranking of real flood events according to their severity based on a consistent assessment of potential impacts. Since effects of flood protection and private precaution were not considered in the models, the ranking differs from the observed actual impacts of the events. For a reanalysis of past flood events, currently used data and models have to be further improved, in particular with regard to elevation data, and validated. For this, procedures for consistent event documentation have to be developed and implemented.

The analysis further shows that homogeneous discharge/hazard scenarios lead to an overestimation of the flood loss probability in large catchments. Large-scale risk management problems should therefore be approached by using heterogeneous flood hazard scenarios that better represent real flood situations. It is acknowledged that reinsurers are well aware of this finding. Still, more scientifically based methods need to be developed, tested and applied to derive real flood situations in large catchments or along large river reaches. To assess whether homogeneous hazard scenarios might still be used to assess real flood situations in a given area, correlations between discharge gauging stations should be calculated, and it should be investigated whether distinct flood pattern can be distinguished in the area under study. Availability of (long) discharge records might, however, restrict such investigations.

ACKNOWLEDGEMENTS

This research was performed at the GFZ Potsdam and funded by AON Re Hamburg from 2004 to 2006. Support on the implementation of the hydraulic model by our colleague Falko

Theisselmann is gratefully acknowledged. Comments given by two anonymous reviewers greatly improved a former version of this manuscript.

REFERENCES

Apel, H., Thieken, A.H., Merz, B. and Blöschl, G. (2004) Flood Risk Assessment and Associated Uncertainty. *Nat. Hazards Earth Syst. Sci.*, **4**, 295-308.

Apel, H., Thieken, A.H., Merz, B. and Blöschl, G. (2006) A probabilistic modelling system for assessing flood risks. *Nat. Hazards*, **38**(1-2), 79-100.

Apel, H., Merz, B. and Thieken, A.H. (2008) Quantification of uncertainties in flood risk assessments. *Journal of River Basin Management*, **6**(2), 149-162.

Apel, H., Aronica, G.T., Kreibich, H. and Thieken, A.H. (2009) Flood risk analyses – how detailed do we need to be? *Nat. Hazards*, **49**, 79-98.

Arnell, N.W. (1989) Expected Annual Damages and Uncertainties in Flood Frequency Estimation. *Journal of Water Resources Planning and Management*, **115**(1): 94-107.

Bubeck, P., Botzen, W.J.W., Kreibich, H. and Aerts, J.C.J.H. (2012) Long-term development and effectiveness of private flood mitigation measures: an analysis for the German part of the river Rhine. *Nat. Hazards Earth Syst. Sci.*, **12**, 3507–3518.

Büchele, B., Kreibich, H., Kron, A., Thieken, A., Ihringer, J., Oberle, P., Merz, B. and Nestmann, F. (2006) Flood-risk mapping: contributions towards an enhanced assessment of extreme events and associated risks. *Nat. Hazards Earth Syst. Sci.*, **6**(4), 485-503.

Castellarin, A., Kohnová, S., Gaál, L., Fleig, A., Salinas, J.L., Toumazis, A., Kjeldsen, T.R., Macdonald, N. (2012): Review of applied statistical methods for flood-frequency analysis in Europe. Centre for Ecology & Hydrology. FloodFreq COST Action ES0901, available at http://www.cost.eu/library/publications/12-28-Review-of-Applied-Statistical-Methods-For-Flood-Frequency-Analysis-in-Europe (accessed on 8 May 2013).

Changnon, S.A. (2003) Shifting Economic Impacts from Weather Extremes in the United States: A Result of Societal Changes, not Global Warming. *Natural Hazards*, **29**, 273-290.

Cullen, A.C. and Frey, H.C. (1999) *Probabilistic Techniques in Exposure Assessment – A Handbook for Dealing with Variability and Uncertainty in Models and Inputs*. Plenum Press, New York.

Disse, M. and Engel, H. (2001) Flood Events in the Rhine Basin: Genesis, Influences and Mitigation. *Nat. Hazards*, **23**, 271-290.

Downton M.W. and Pielke R.A. Jr. (2005) How accurate are disaster loss data? The case of U.S. flood damage. *Nat. Hazards*, **35**, 211–228.

DVWK (1999) *Statistische Analyse von Hochwasserabflüssen*, Wirtschafts- und Verlags-Ges. Gas. und Wasser, Bonn.

Elmer, F., Kreibich, H., Seifert, I. and Thieken, A.H. (2010) A Delphi-method expert survey to derive standards for flood damage data collection. *Risk Anal.*, **30**(1), 107-124.

Gall, M., Borden, K. and Cutter, S.L. (2009): When do losses count? Six fallacies of loss data from natural hazards. *BAMS*, **90**(6), 1-11.

Gallego, J. (2001) Using land cover information to map population density. In Statistical Commission and Economic Commission for Europe (eds.) *Conf. of European Statisticians*, Working Paper No. 21, 1–10, Tallinn, Estonia.

Ghizzoni, T., Roth, G. and Rudari, R. (2012) Multisite flooding hazard assessment in the Upper Mississippi River. *J. Hydrol.*, **412-413**, 101-113.

Ghizzoni, T., Roth, G. and Rudari, R. (2010) Multivariate skew-t approach to the design of accumulation risk scenarios for the flooding hazard. *Adv. Water Res.*, **33**, 1243-1255.

Gouldby, B., Samuels, P., Klijn, F., Messner, F., van Os,A., Sayers, P. and Schanze, J. (2005) Language of Risk – Project Definitions. FloodSite-Report: T32-04-01, http://www.floodsite.net/html/partner_area/project_docs/FLOODsite_Language_of_Risk_v4_0_P1.pdf (last access: 28 November 2012)

Greenberg, M.R., Lahr, M. and Mantell, N. (2007) Understanding the Economic Costs and Benefits of Catastrophes and Their Aftermath: A Review and Suggestions for the U.S. Federal Government. *Risk Anal.*, **27**(1), 83-96.

Grothmann, T. and Reusswig, F. (2006) People at Risk of Flooding: Why Some Residents Take Precautionary Action While Others do not. *Nat. Hazards*, **38**, 101–120.

Hall J. and Anderson M. (2002) Handling uncertainty in extreme unrepeatable hydrological processes – the need for an alternative paradigm. *Hydrol. Process.*, **16**, 1867–1870.

Handmer, J., Abrahams, J., Betts, R. and Dawson, M (2005) Towards a consistent approach to disaster loss assessment across Australia. The Australian Journal of Emergency Management, **20**(1), 10-18.

Heffernan, J.E. and Tawn, J.A. (2004) A conditional approach for multivariate extreme values. *Journal Royal Statistical Society B*, **66**, 497-546.

Hosking, J.R.M. and Wallis, J.R. (1997) *Regional Frequency Analysis: An Approach Based on L-Moments*. Cambridge University Press, Cambridge.

ICPR – International Commission for the Protection of the river Rhine (2001) Rhine-Atlas [online]. ICPR, Koblenz, http://www.iksr.org/fileadmin/user_upload/Dokumente_de/Rhein-Atlas/Start.pdf (accessed 18 November 2012).

Kaplan, S. and Garrick, B.J. (1981) On the quantitative definition of risk. *Risk Anal.*, **1**, 11-27.

Keef, C., Svensson, C. and Tawn, J. A. (2009a) Spatial dependence in extreme river flows and precipitation for Great Britain. *Journal of Hydrology*, **378**, 240-252.

Keef, C., Tawn, J. A. and Svensson, C. (2009b) Spatial risk assessment for extreme river flows. *Journal Royal Statistical Society C*, **58**, 601-618.

Kleist, L., Thieken, A.H., Köhler, P., Müller, M., Seifert, I., Borst, D. and Werner, U. (2006): Estimation of the regional stock of residential buildings as a basis for comparative risk assessment for Germany. *Nat. Hazards Earth Syst. Sci.*, **6**(4): 541-552.

Kron, W., Steuer, M., Löw, P. and Wirtz, A. (2012) How to deal properly with a natural catastrophe database – analysis of flood losses. *Nat. Hazards Earth Syst. Sci.*, **12**, 535–550.

Lammersen, R., Engel, H., van de Langemheen, W. and Buiteveld, H. (2002) Impact of river training and retention measures on flood peaks along the Rhine. *J. Hydr.*, **267**, 115–124.

Merz, B. and Thieken, A.H. (2005) Separating Natural and Epistemic Uncertainty in Flood Frequency Analysis. – *Journal of Hydrology*, **309**, 114-132.

Merz, B. and Thieken, A.H. (2009) Flood risk curves and uncertainty bounds. *Natural Hazards*, **51**(3), 437-458.

Merz, B., Thieken, A.H. and Apel, H. (2005) What can go wrong? Flood risk assessment and scenario analysis. In van Alphen, J., van Beek, E. and Taal, M. (Eds.) *Floods, from Defence to Management*, p. 673-679. Taylor & Francis Group, London.

Merz, B., Elmer, F. and Thieken, A. H. (2009) Significance of “high probability/low damage” versus “low probability/high damage” flood events. *Nat. Hazards Earth Syst. Sci.*, **9**, 1033-1046.

Merz, B., Kreibich, H., Schwarze, R. and Thieken, A. (2010) Review article „Assessment of economic flood damage“. *Nat. Hazards Earth Syst. Sci.*, **10**, 1697-1724.

Mileti, D.S. (1999) *Disasters by design: a reassessment of natural hazards in the United States*. Joseph Henry, Washington DC.

Ramirez, J., Adamowicz, W.L., Easter, K.W. and Graham-Tomasi, T. (1988) Ex post analysis of flood control: Benefit-cost analysis and the value of information. *Water Resour. Res.*, **24**, 1397-1405.

Rodda, H.J.E. (2005) The development and application of a flood risk model for the Czech Republic. *Nat. Hazards*, **36**, 207–220.

Rodda, H. J. E. and Berger, A. (2002) The application of flood modelling and mapping for managing flood risk in the UK. In Spreafico, M. and Weingartner, R (eds.) *International Conference on Flood Estimation*, p. 645-650, Berne, CHR. Report II-17.

Romanowicz, R. and Beven, K. (2003) Estimation of flood inundation probabilities as conditioned on event inundation maps. *Water Resour. Res.*, **39,** W01073.

Schwarze, R. and Wagner, G.G. (2004) In the Aftermath of Dresden: New Directions in German Flood Insurance. *The Geneva Papers on Risk and Insurance*, **29**, 154-168.

Stedinger, J.R., Vogel, R.M. and Foufoula-Georgiou, E. (1992) Frequency analysis of extreme events. In Maidment, D.R. (Ed.) *Handbook of Hydrology* pp. 18.1–18.66. McGraw-Hill, New York.

te Linde, A.H., Aerts, J.C.J.H. and Kwadijk, J.C.J. (2010) Effectiveness of flood management measures on peak discharges in the Rhine basin under climate change. *J. Flood Risk Man.,* **3**, 248-269.

te Linde, A.H., Bubeck, P., Dekkers, de Moel, H. and Aerts, J.C.J.H (2011) Future flood risk estimates along the river Rhine. *Nat. Hazards Earth Syst. Sci.*, **11**, 459-473.

Thieken, A.H., Müller, M., Kleist, L., Seifert, I., Borst, D. and Werner, U. (2006) Regionalisation of asset values for risk analyses. *Nat. Hazards Earth Syst. Sci*, **6**(2), 167-178.

Thieken, A.H., Olschewski, A., Kreibich, H., Kobsch, S. and Merz, B. (2008) Development and evaluation of FLEMOps – a new Flood Loss Estimation MOdel for the private sector. In

Proverbs, D., Brebbia, C.A. and Penning-Rowsell, E. (eds.): *Flood Recovery, Innovation and Response*, p. 315-324, WIT Press.

Thieken, A. (2011) Methods for the documentation and estimation of direct flood losses. In Zenz, G. and Hornich, R. (Eds.) *Urban Flood Risk Management – Approaches to enhance resilience of communities*. p. 479-484. Graz.

Uhlemann, S., Thieken, A.H. and Merz, B. (2010) A consistent set of trans-basin floods in Germany between 1952 - 2002. *Hydrol. Earth Syst. Sci.*, **14**, 1277–1295.

USACE (1999) Risk-Based Analysis in Geotechnical Engineering for Support of Planning Studies. Engineer Technical Letter (ETL) 1110–2-556, U.S. Army Corps of Engineers, Washington D.C.

Van Dyck, J. and Willems, p. (2013): Probabilistic flood risk assessment over large geographical areas. Accepted article for Water Resources Research, doi: 10.1002/wrcr.20149.

Vogel, R.M., McMahin, T.A. and Chiew, F.H.S. (1993) Floodflow frequency model selection in Australia. *J Hydro.*, **146**, 421-449.

Vogel, R.M. and Wilson, I. (1996) Probability Distribution of Annual Maximum, Mean, and Minimum Streamflows in the United States. *J. Hydrol. Engineering*, **1**, 69-76.

Vorogushyn, S., Merz, B., Lindenschmidt, K.-E. and Apel, H. (2010) A new methodology for flood hazard assessment considering dike breaches. *Water Resour. Res.*, **46**, W08541.

Wind, H.G, Nierop, T.M., de Blois, C.J. and de Kok, J.L. (1999) Analysis of flood damages from the 1993 and 1995 Meuse flood. *Water Resour. Res.*, **35**(11), 3459-3465.

Wünsch, A., Herrmann, U., Kreibich, H. and Thieken, A.H. (2009) The Role of Disaggregation of Asset Values in Flood Loss Estimation: A Comparison of Different Modeling Approaches at the Mulde River, Germany. *Environ. Man.*, **44**(3), 524-541.

Total number of words: 9118